Articles

Contribution No. 7739 from the Arthur Amos Noyes Laboratories, Division of Chemistry and Chemical Engineering, California Institute of Technology, Pasadena, California 91125, and Research School of Chemistry, The Australian National University, G.P.O. Box 4, Canberra 2601, Australia

Autoxidation of the (Sarcophagine)ruthenium(2+) Complex Involving Hydrogen Atom Transfer to O_2^-

Paul Bernhard,[†] Alan M. Sargeson,[‡] and Fred C. Anson*,[†]

Received February 19, 1988

The autoxidation of the $Ru(sar)^{2+}$ complex (Figure 1; sar = 3,6,10,13,16,19-hexaazabicyclo[6.6.6]eicosane), in which the metal center is encapsulated, has been studied by a combination of electrochemical and spectrophotometric techniques. The rate of the autoxidation exhibits a pronounced pH dependence in the range $2.5 < pH < 11$. The rate law in acid (pH <2.5) is first order in both $[Ru(sar)^{2+}]$ and $[O_2]$, and the pH-independent rate constant ($k_0 = 1.4 \pm 0.1$ M^{-1} s^{-1}, $T = 25$ °C, $\mu = 0.1$ M) fits well into a series of previously studied Ru(II) amine complexes. At pH >11 the rate law is also first order with respect to both $[Ru(sar)^{2+}]$ and $[O_2]$ but the pH-independent rate constant is significantly larger ($k_b = 33.4 \pm 1.0$ M^{-1} s^{-1}, $T = 25$ °C, $\mu = 0.1$ M). A mechanism is presented to account for the difference in rate constant at low and at high pH. The mechanism in base features the transfer of a hydrogen atom from the $Ru(sar)^{2+}$ complex to the superoxide radical, O_2^-, to form directly a deprotonated Ru(III) species that reacts rapidly with O_2 to form another O_2^- radical and a long-lived Ru(IV) complex ($t_{1/2} \approx 15$ min). In the intermediate-pH region, where no analytical expression for the rate law is available because of the complexity of the reaction pattern, the mechanism correctly predicts the small observed deviations from first-order behavior. Important parameters obtained from an analysis of the kinetic data are an extraordinarily low pK_a of ca. 6.3 for the proton on the secondary nitrogen atom in $Ru(sar)^{3+}$ and a formal potential of +0.05 V (vs NHE) for the singly deprotonated $Ru^{IV/III}(sar(-H^+))^{3+/2+}$ couple. Implications of the mechanism for other systems are discussed.

Introduction

The reduction of dioxygen and the oxidation of superoxide by transition-metal complexes have been the focus of a number of recent studies,[1-4] but some aspects of the mechanisms remain obscure. For instance, although the rates of the autoxidation of a series of Ru(II) amine complexes[1a] exhibited the linear dependence on driving force expected from the Marcus theory[5] for outer-sphere electron-transfer reactions, calculation of the electron self-exchange rate constant for the O_2/O_2^- couple (from cross reactions with other reaction partners by the application of the Marcus cross relation) leads to values that range over 10 orders of magnitude.[4] The origin of this disparate behavior remains to be elucidated, although it is likely that solvation effects are important.[6] It is also not clear that a distinction between inner-sphere and outer-sphere reactions can be maintained in the cases of O_2 and O_2^-. Taube has pointed out[7] that O_2^- has an affinity for metal ions (well documented in the case of cobalt[8]) that is larger than is expected from comparisons with other small oxygen-donor ligands and from the relatively moderate Brønsted basicity of O_2^- ($pK_{HO_2} = 4.7$[10]). This factor and their small sizes may allow O_2 and O_2^- to interact with the d orbitals of transition metals even in cases where the complexes are coordinatively saturated. Such interactions could allow O_2 and O_2^- to bridge the gap between cleanly outer-sphere and inner-sphere reactants.

Another unsettled issue in autoxidations of transition metals is the fate of the superoxide anion that is usually generated in the first step. Protonation leads to the powerful oxidant HO_2 ($E^f(HO_2/H_2O_2) = 1.44$ V vs NHE[9]), which is usually rapidly reduced by mechanisms that are themselves poorly understood.[1b] HO_2 and O_2^- engage in a rapid dismutation reaction to produce O_2 and HO_2^-, but O_2^- is generally not an outer-sphere oxidant in aqueous solution because the resulting O_2^{2-} anion is highly unstable.[11] The stable HO_2^- anion is, however, potentially accessible by means of an H atom transfer reaction. In a recent study,[2a] evidence in support of H atom abstraction by O_2^- from $Co(sep)^{2+}$ (sep = sepulchrate = 1,3,6,8,10,13,16,19-octaazabicyclo[6.6.6]eicosane) was presented and reactions of O_2^- with certain organic hydrogen atom donors have also been reported.[12]

The present study was initially undertaken to compare the rates of autoxidation of two Ru(II) complexes, $Ru(sar)^{2+}$ (sar = sarcophagine = 3,6,10,13,16,19-hexaazabicyclo[6.6.6]eicosane; Figure 1) and $Ru(tacn)_2^{2+}$ (tacn = 1,4,7-triazacyclononane), with those of more familiar Ru(II) amine complexes. However, in the course of the experiments a peculiar dependence of the rate upon pH and the concentrations of the reactants was observed for the $Ru(sar)^{2+}$ complex. This prompted the additional experiments that pointed to a mechanism which is discussed in what follows. The thermodynamic and kinetic properties of the $Ru(sar)^{2+}$ complex had previously been studied in some detail,[13] which led to a valuable reduction in the number of unknown parameters employed in the analysis of the kinetics.

Experimental Section

A. Syntheses and Materials. Water was purified by passage through a Barnstead Nanopure train. $LiCF_3SO_3$ was prepared by neutralizing

[†] California Institute of Technology.
[‡] The Australian National University.

(1) (a) Stanbury, D. M.; Haas, O.; Taube, H. *Inorg. Chem.* **1980**, *19*, 518. (b) Stanbury, D. M.; Mulac, W. A.; Sullivan, J. C.; Taube, H. *Inorg. Chem.* **1980**, *19*, 3735. (c) Anson, F. C.; Ni, C.-L.; Saveant, J.-M. *J. Am. Chem. Soc.* **1985**, *107*, 3442.
(2) (a) Bakac, A.; Espenson, J. H.; Creaser, I. I.; Sargeson, A. M. *J. Am. Chem. Soc.* **1983**, *105*, 7624. (b) Creaser, I. I.; Geue, R. J.; Harrowfield, J. M.; Herlt, A. J.; Sargeson, A. M.; Snow, M. R.; Springborg, J. *J. Am. Chem. Soc.* **1982**, *104*, 6016.
(3) Bradic, Z.; Wilkins, R. G. *J. Am. Chem. Soc.* **1984**, *106*, 2236 and references therein.
(4) McDowell, M. S.; Espenson, J. H.; Bakac, A. *Inorg. Chem.* **1984**, *23*, 2232 and references therein.
(5) Marcus, R. A. *Annu. Rev. Phys. Chem.* **1964**, *15*, 155.
(6) Hill, H. A. O. In *Oxygen Free Radicals and Tissue Damage*; Elsevier: Amsterdam, 1979; p 54.
(7) Taube, H. *Prog. Inorg. Chem.* **1986**, *34*, 607.
(8) Wong, C. L.; Switzer, J. A.; Balakrishnan, P. K.; Endicott, J. F. *J. Am. Chem. Soc.* **1980**, *102*, 5511.
(9) Fee, J. A.; Valentine, J. S. In *Superoxide and Superoxide Dismutase*; Michelson, A. M., McCord, J. M., Fridovich, I., Eds.; Academic: New York, 1977; pp 19-60.
(10) Bielski, B. H. J. *J. Photochem. Photobiol.* **1978**, *28*, 645.
(11) Sawyer, D. T.; Valentine, J. S. *Acc. Chem. Res.* **1981**, *14*, 393.
(12) (a) Bielski, B. H. J.; Richter, H. W. *J. Am. Chem. Soc.* **1977**, *99*, 3019. (b) Nanni, E. J.; Sawyer, D. T. *J. Am. Chem. Soc.* **1980**, *102*, 7591.
(13) (a) Bernhard, P.; Sargeson, A. M. *J. Chem. Soc., Chem. Commun.* **1985**, 1516. (b) Bernhard, P.; Sargeson, A. M. *Inorg. Chem.* **1987**, *26*, 4122. (c) Bernhard, P.; Sargeson, A. M., submitted for publication in *J. Am. Chem. Soc.*

0020-1669/88/1327-2754$01.50/0

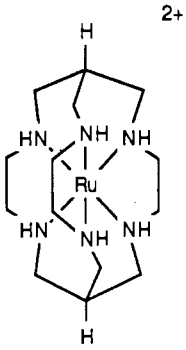

1

$Ru(sar)^{2+}$

Figure 1. Structure of the $Ru(sar)^{2+}$ complex.

CF_3SO_3H (distilled at reduced pressure before use) with LiOH (Merck p.A.) and dried at 140 °C overnight. $NaClO_4$, the buffers MES (2-morpholinoethanesulfonic acid) and HEPES (*N*-(2-hydroxyethyl)-piperazine-*N'*-ethanesulfonic acid) and KO_2 were used without further purification. $[Ru(sar)](CF_3SO_3)_2$ was synthesized as reported previously.[13a] pH measurements were carried out with an Orion pH meter using a combination electrode calibrated at pH 4 and 7.

B. Kinetic Measurements. Half-lives for the autoxidation of $Ru(sar)^{2+}$ (eq 1) in the pH range 0–12 varied between 20 s and 20 min when the solution was saturated with O_2($[O_2] = 1.1 \times 10^{-3}$ M[14]) or air ($[O_2] = 0.23 \times 10^{-3}$ M).

$$2Ru(sar)^{2+} + O_2 + 2H^+ \rightarrow 2Ru(sar)^{3+} + H_2O_2 \quad (1)$$

The product of the oxidation, $Ru(sar)^{3+}$, is unstable in aqueous solution, where, following deprotonation, it disproportionates to form $Ru(sar)^{2+}$ and a Ru(IV) complex that is subsequently and irreversibly converted to a Ru(II) imine complex[13c] (eq 2 and 3) (which also reacts with O_2, but more slowly). sar($-H^+$) represents the deprotonated sar ligand, and imsar represents the oxidized, imine form of the ligand. The spectral changes resulting from this chemistry were too complex to allow the kinetics to be followed spectrophotometrically (except at high pH). For this reason an electrochemical method[1c] was employed to monitor continuously the concentration of $Ru(sar)^{2+}$. The setup consisted of conventional electrochemical instrumentation and a thermostated cell (25 ± 0.2 °C) equipped with a freshly cleaved basal plane graphite rotating disk electrode that was rotated at 1000–4000 rpm. A voltammogram was first recorded to determine the potential of the $Ru(sar)^{2+}$ oxidation wave at each pH. The rotating electrode was then kept at a potential on the plateau of the $Ru(sar)^{2+}$ oxidation wave, where the $Ru^{II}(imsar)^{2+}$ complex produced in reaction 3 is not electroactive.[15] Potentials were measured with respect to a sodium chloride saturated calomel electrode but are quoted vs NHE.

$$Ru(sar)^{3+} + Ru^{III}(sar(-H^+))^{2+} \rightleftharpoons Ru(sar)^{2+} + Ru^{IV}(sar(-H^+))^{3+} \quad (2)$$

$$Ru^{IV}(sar(-H^+))^{3+} \rightarrow Ru^{II}(imsar)^{2+} + H^+ \quad (3)$$

In a typical kinetic experiment a 0.2-mL aliquot of a $Ru(sar)^{2+}$ stock solution was injected into 15 mL of a test solution adjusted to an ionic strength of 0.1 M with $LiCF_3SO_3$ or $NaClO_4$ and saturated with oxygen or air. The decreasing anodic disk current was monitored as the $Ru(sar)^{2+}$ was consumed by reaction with O_2. Oxygen or air was continuously bubbled through the solution during the experiment to maintain a constant concentration of O_2. The gas inlet was positioned above the disk electrode to minimize perturbations in the current from bubbles. The reaction half-lives were sufficiently short that the amount of $Ru(sar)^{2+}$ consumed by reaction at the disk was negligible.

At pH 10 and above the reaction could also be conveniently followed spectrophotometrically because the Ru(IV) product exhibited a strong absorbance at 430 nm (Figure 5) before it was slowly ($t_{1/2} \approx 15$ min) converted to the Ru(II) imine species by reaction 3.

The current–time data were fitted to the first-order expression given in eq 4, where i_0 and i_∞ are the currents at the beginning and at the end of a run, respectively. Spectrophotometric absorbance–time data were fitted to an analogous equation. At pH <2.5 or pH >11 the reaction exhibited clear first-order behavior with respect to the concentrations of $Ru(sar)^{2+}$ and O_2, but at the intermediate pH values slight deviations from first-order behavior were observed. Calculations were performed on a VAX 11/750 computer using the least-squares routine ZXSSQ of the International Math Subroutine Library (IMSL).

$$i(t) = i_\infty + (i_0 - i_\infty) \exp(-k_{obsd}t) \quad (4)$$

(14) Seidell, A.; Linke, W. F. *Solubilities of Inorganic Compounds*, 4th ed.; Van Nostrand: Princeton, NJ, 1964; p 1228.

(15) The formal potential of the $Ru(imsar)^{3+/2+}$ couple is ca. 0.15 V more positive than that of the $Ru(sar)^{3+/2+}$ couple.[13c]

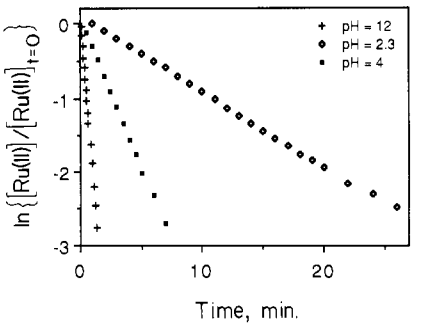

Figure 2. Pseudo-first-order kinetic plots for the autoxidation of $Ru(sar)^{2+}$. The concentration of $Ru(sar)^{2+}$ was monitored electrochemically at pH 2.3 and 4 and spectrophotometrically at pH 12. All solutions were kept saturated with O_2. The initial concentrations of $Ru(sar)^{2+}$ were 1.4×10^{-4}, 2.2×10^{-5}, and 6.6×10^{-5} M at pH 2.3, 4, and 12, respectively.

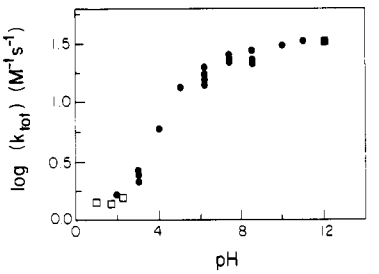

Figure 3. pH dependence of the second-order rate constant for the autoxidation of $Ru(sar)^{2+}$ (eq 5 and 6). Ionic strength was maintained at 0.1 M with $LiCF_3SO_3$ (□) or $NaClO_4$ (●). Buffers employed (see Experimental Section) were MES (pH 5.1, 6.2) and HEPES (pH 7.5, 8.5).

Results

The structure of the $Ru(sar)^{2+}$ complex examined in this study is shown in Figure 1. One of the most interesting features in the kinetics of its autoxidation is the pronounced dependence of the rate upon pH: At pH 11 or higher the reaction is 25 times faster than at pH 2.5 or lower. Such behavior is highly unusual for the autoxidation of transition-metal complexes, so we examined the kinetics in some detail. The autoxidation reaction appeared to be first order in $Ru(sar)^{2+}$ at all pH values, and the slopes of plots such as those in Figure 2 yield values of the pseudo-first-order rate constant, k_{obsd}, that increase with the concentration of O_2 as expected for a reaction that is first order with respect to $[O_2]$:

$$\text{rate} = k_{obsd}[Ru(sar)^{2+}] \quad (5)$$

$$k_{obsd} = k_{tot}[O_2] \quad (6)$$

Table I summarizes the second-order rate constants, k_{tot}, evaluated under a variety of reaction conditions in the pH range between 0 and 12. In Figure 3 a plot of log k_{tot} versus pH is shown. In sufficiently acidic or sufficiently basic solutions k_{tot} becomes independent of pH and the transition between these two regions occurs at pH ~4.8. Note that at pH 12 the values of k_{tot} in Table I obtained by the two different analytical methods are in good agreement and that changes in the supporting electrolytes employed produce negligible effects on the rate constants.

The apparent linearity of the plots in Figure 2 suggests simple first-order dependence on $[Ru(sar)^{2+}]$. However, the data in Table I at intermediate pH values, e.g. at pH 6.2, show that k_{tot} exhibits slight but systematic dependences on $[Ru(sar)^{2+}]$ and on $[O_2]$. Increases in $[Ru(sar)^{2+}]$ by factors of 2 and 5 lead to decreases in k_{tot} by 15% and 30%, respectively. A similar dependence of k_{tot} on $[O_2]$ is also observed but with the opposite sign. These

Table I. Kinetic Data for the Autoxidation of $Ru(sar)^{2+}$ (μ = 0.1 M, T = 25 °C)

pH	$10^5[Ru^{2+}]$, M	$10^3[O_2]$, M	k_{tot},[a] M^{-1} s^{-1}	k_{calcd},[b] M^{-1} s^{-1}	method[g]
0.00[c]	13.5	1.1	≈1.1		EC
	6.3	1.1	≈1.2		EC
1.00	13.0	1.1	1.39	1.46	EC
1.70[d]	25.3	1.1	1.35	1.50	EC
2.00[e]	10.1	1.1	1.57	1.63	EC
	7.2	1.1	1.69	1.67	
	11.0	1.1	1.65	1.62	
2.30[d]	14.3	0.23	1.62	1.52	EC
	33.0	1.1	1.57	1.58	
	14.6	1.1	1.53	1.66	
3.00[e]	4.6	1.1	2.59	2.45	EC
	5.0	1.1	2.43	2.41	
	7.1	1.1	2.10	2.25	
4.00[e]	2.2	1.1	6.00	5.93	EC
5.07[e]	2.9	1.1	13.4	11.55	EC
6.22[e]	2.3	1.1	19.9	17.87	EC
	4.6	1.1	17.4	17.26	
	11.7	1.1	15.6	15.74	
	3.1	0.23	14.0	15.21	
7.41[e]	2.9	1.1	25.2	28.20	EC
	5.7	1.1	23.9	27.99	
	8.5	1.1	21.7	27.78	
8.50[e]	2.9	1.1	27.4	32.81	EC
	5.7	1.1	23.2	32.78	
	8.5	1.1	21.5	32.75	
10.00[e]	2.4	1.1	30.2	33.38	VIS
11.00[e]	4.6	1.1	33.0	33.40	VIS
12.00[e]	2.0	0.23	34.4	33.40	VIS
	6.4	1.1	32.4	33.40	
	3.3	1.1	34.4	33.40	
12.00[d]	2.7	1.1	36.0	33.40	VIS
	4.4	1.1	30.4	33.40	
	8.7	1.1	33.6	33.40	
12.00[e]	3.5	1.1	33.7	33.40	EC
	5.7	1.1	33.8	33.40	
	8.7	1.1	33.6	33.40	
12.00[e,f]		1.1	20.5		VIS

[a] $k_{tot} = k_{obsd}/[O_2]$; average reproducibility was ca. ±10%. [b] Calculated (eq 22, 28) with pK_{III} = 6.3, k_5/k_2 = 66.30, k_4/k_2 = 1.93 × 10^4, and k_1/k_2 = 60 (for definitions of rate constants see Schemes I and II). [c] 1.0 M CF_3SO_3H. [d] Ionic strength adjusted to 0.1 M with CF_3SO_3Li. [e] Ionic strength adjusted to 0.1 M with $NaClO_4$. [f] In D_2O. [g] Abbreviations: EC, electrochemistry, disappearance of $Ru(sar)^{2+}$; VIS, spectroscopy, appearance of $Ru^{IV}(sar(-2H^+))^{2+}$.

deviations from pure second-order kinetics at intermediate pH values will be shown to be consistent with the explanation we will offer to account for the pH dependence of k_{tot}. However, the deviations were always small and we neglected them in evaluating rate constants from plots such as those in Figure 2.

Behavior in 1 M CF_3SO_3H. The kinetics of the autoxidation of $Ru(sar)^{2+}$ are complicated by the disproportionation of the first oxidation product, $Ru(sar)^{3+}$, according to reaction 2.[13c] At pH ≥1 the disproportionation reaction was sufficiently rapid under the conditions employed that $Ru(sar)^{3+}$ was not observed as an intermediate. However, in 1 M CF_3SO_3H the appearance and disappearance of $Ru(sar)^{3+}$ could be readily observed by adjusting the potential of the rotating-disk electrode to 0.1 V vs NHE, where the only electrode reaction occurring is the reduction of $Ru(sar)^{3+}$ to $Ru(sar)^{2+}$. The disk current–time response obtained under these conditions is shown in Figure 4. The concentration of $Ru(sar)^{3+}$ increases for about 8 min and then gradually decreases to zero as the disproportionation reaction slowly ensues. The disproportionation is relatively unimportant during the initial, rising portion of the current–time curve from which the value of k_{tot} listed in Table I for pH 0 was evaluated.

Behavior at pH 12. When the autoxidation was carried out in 0.01 M NaOH, the only detectable product was a complex with a strong absorbance at 430 nm (ϵ_{max} = 8000 M^{-1} cm^{-1}) (Figure 5), which slowly converted ($t_{1/2} \simeq$ 15 min) to the Ru(II) imine complex. The latter process was not studied in detail although qualitative experiments showed that the rate of conversion was

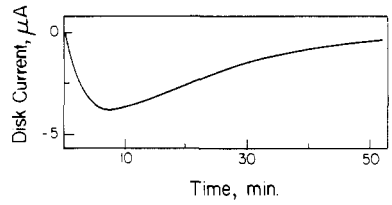

Figure 4. Cathodic current–time response obtained at a rotating-disk electrode maintained at +0.1 V vs NHE during the autoxidation of $Ru(sar)^{2+}$ in 1 M CF_3SO_3H. The initial concentration of $Ru(sar)^{2+}$ was 1.35 × 10^{-4} M. The solution was kept saturated with O_2.

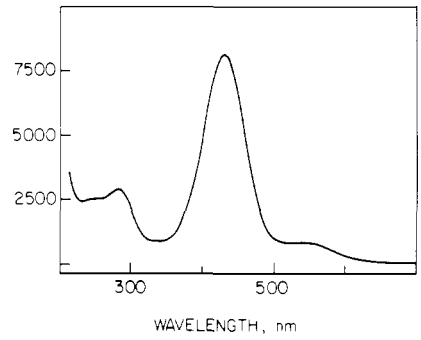

Figure 5. Spectrum of the $Ru^{IV}(sar(-2H^+))^{2+}$ complex resulting from the autoxidation of $Ru(sar)^{2+}$ at pH 12. The ordinate is molar absorbance.

substantially faster at lower pH, implying acid catalysis. The spectrum in Figure 5 is very similar to that of the much shorter lived, monodeprotonated $Ru^{IV}(sar(-H^+))^{3+}$ complex (λ_{max} = 445 nm; ϵ_{max} = 7800 M^{-1} cm^{-1}), which was identified in a previous study.[13c] These observations are consistent with the assignment of the spectrum in Figure 5 to a doubly deprotonated Ru(IV) amine complex. Electrochemical measurements helped to bolster this interpretation. Solutions giving rise to the spectrum in Figure 5 exhibit cyclic voltammograms with the same, reversible, pH-dependent couple as that observed with solutions of $Ru(sar)^{2+}$ at the same pH. The voltammetric response corresponds to a two-electron process with a formal potential that decreases by 59 mV per unit change in pH. The electrode process can be ascribed to half-reaction 7, which has a formal potential of −0.26 V vs NHE at pH 12.

$$Ru^{IV}(sar(-2H^+))^{2+} + 2e^- + 2H^+ \rightleftharpoons Ru(sar)^{2+} \quad (7)$$

The hydrogen peroxide produced in the autoxidation of $Ru(sar)^{2+}$ was readily observed at pH 12, where the O_2/HO_2^- couple exhibits a reversible cyclic voltammetric response at mercury electrodes.

$Ru(sar)^{2+}$ is much less reactive toward H_2O_2 than toward O_2. This was demonstrated at pH 12, where mixtures of $Ru(sar)^{2+}$ and H_2O_2 (or $Ru^{IV}(sar(-2H^+))^{2+}$ and O_2) continued to exhibit two separate responses at +0.12 and −0.26 V, corresponding to the O_2/HO_2^- and $Ru^{IV}(sar(-2H^+))^{2+}/Ru(sar)^{2+}$ couples, respectively, for time periods (e.g. 5 min) that were much longer than those required for the autoxidation to reach completion.

Mechanism of the Autoxidation. To arrive at a possible mechanism for the autoxidation process, it is useful to summarize in reactions 2 and 8–10 some of the thermodynamic and kinetic parameters for the ruthenium sarcophagine complexes that are available from previous studies.[13]

$$Ru(sar)^{3+} + e^- \rightleftharpoons Ru(sar)^{2+} \qquad E^f_{3/2} = 0.29 \text{ V} \quad (8)$$

$$Ru(sar)^{3+} \rightleftharpoons Ru^{III}(sar(-H^+))^{2+} + H^+ \qquad pK_{III} \approx 5\text{–}7 \quad (9)$$

$$Ru^{IV}(sar(-H^+))^{3+} + e^- \rightleftharpoons Ru^{III}(sar(-H^+))^{2+} \qquad E^f_{IV/III} \approx 0.05\text{–}0.15 \text{ V} \quad (10)$$

$$Ru(sar)^{3+} + Ru^{III}(sar(-H^+))^{2+} \underset{k_{-d}}{\overset{k_d}{\rightleftharpoons}} Ru(sar)^{2+} + Ru^{IV}(sar(-H^+))^{3+} \quad (2)$$

$$K_{III}k_d = 37 \pm 1 \text{ s}^{-1} \qquad k_{-d} = 6.2 \times 10^3 \text{ M}^{-1} \text{ s}^{-1}$$

$Ru(sar(-H^+))$ and $Ru(sar(-2H^+))$ denote complexes in which one and two protons, respectively, have dissociated from the secondary nitrogen atoms of the coordinated sar ligand.[13c] We will first consider the limiting cases at low and high pH, where the rate constant k_{tot} is independent of pH (Figure 2).

Kinetics at pH <2.5. For the acidic limit it seems appropriate to consider the mechanism proposed by Stanbury et al.[1a] for the one-electron autoxidation of simple Ru(II) amine complexes as modified to incorporate the spontaneous disproportionation of $Ru(sar)^{3+}$ (Scheme I).

Scheme I

$$Ru(sar)^{2} + O_2 \rightarrow Ru(sar)^{3+} + O_2^- \quad k_0 \qquad (11)$$

$$O_2^- + H^+ \rightleftharpoons HO_2 \quad K_{HO_2}^{-1} \qquad (12)$$

$$Ru(sar)^{2+} + HO_2 \rightarrow Ru(sar)^{3+} + HO_2^- \quad k_1 \qquad (13)$$

$$Ru(sar)^{3+} \rightleftharpoons Ru^{III}(sar(-H^+))^{2+} + H^+ \quad K_{III} \qquad (9)$$

$$Ru(sar)^{3+} + Ru^{III}(sar(-H^+))^{2+} \rightarrow Ru(sar)^{2+} + Ru^{IV}(sar(-H^+))^{3+} \quad k_d \qquad (14)$$

$$Ru^{III}(sar(-H^+))^{2+} + HO_2 \rightarrow Ru^{IV}(sar(-H^+))^{3+} + HO_2^- \quad k_4 \qquad (15)$$

Despite the fact that reaction 11 has an unfavorable equilibrium constant of 3.8×10^{-7}, its reverse has been neglected in Scheme I because of the rapid removal of O_2^- by protonation (reaction 12) and of $Ru(sar)^{3+}$ by reactions 9 and 14. In addition, no evidence of inhibition by reaction products was observed. Back-reactions for all of the other electron-transfer steps were neglected because all have substantial driving forces to proceed from left to right and the observed rates did not exhibit the pH dependences that would result if significant contributions from the reverse of reaction 14 were important.

It was also possible to neglect the disproportionation of superoxide because, at the steady-state concentrations involved, the rates of reaction of O_2^- or HO_2 with $Ru(sar)^{2+}$ or $Ru^{III}(sar(-H^+))^{2+}$ were orders of magnitude more rapid than the second-order disproportionation reaction.

When the steady-state approximation is made for the concentrations of both $(HO_2 + O_2^-)$ and $(Ru(sar)^{3+} + Ru^{III}(sar(-H^+))^{2+})$ with the assumption that all protonation equilibria are rapidly established, it can be shown (see Appendix) that the rate law for Scheme I reduces to the simple second-order form of eq 16 in which reaction 11 alone controls the rate of disappearance

$$-\frac{d[Ru(sar)^{2+}]}{dt} = k_0[Ru(sar)^{2+}][O_2] \qquad (16)$$

of $Ru(sar)^{2+}$. This allows k_0 ($=k_{tot}$) to be evaluated from plots such as those in Figure 2 at $1 < pH < 2.5$ (as well as from the initial portion of the curve in Figure 4 at pH 0). The values obtained are listed in Table I. The best estimate for k_0 was 1.4 $\pm$ 0.1 M^{-1} s^{-1}.

Kinetics at High pH. At pH >10, where the rate constant k_{tot} is greater but also independent of pH, Scheme II seems appropriate.

Scheme II

$$Ru(sar)^{2+} + O_2 \rightarrow Ru(sar)^{3+} + O_2^- \quad k_0 \qquad (11)$$

$$Ru(sar)^{3+} \rightleftarrows Ru^{III}(sar(-H^+))^{2+} + H^+ \quad K_{III} \qquad (9)$$

$$Ru(sar)^{2+} + O_2^- \rightarrow Ru^{III}(sar(-H^+))^{2+} + HO_2^- \quad k_2 \qquad (17)$$

$$Ru^{III}(sar(-H^+))^{2+} + O_2 \rightarrow Ru^{IV}(sar(-H^+))^{3+} + O_2^- \quad k_3 \qquad (18)$$

$$Ru^{III}(sar(-H^+))^{2+} + O_2^- \rightarrow Ru^{IV}(sar(-2H^+))^{2+} + HO_2^- \quad k_5 \qquad (19)$$

The reverse of reaction 11 was neglected because of the rapid removal of $Ru(sar)^{3+}$ by reaction 9 and of O_2^- by reaction 17. Reactions 17–19 were assumed to be irreversible because of their substantial equilibrium constants. Applying the steady-state approximation to both O_2^- and $Ru^{III}(sar(-H^+))^{2+}$ in Scheme II leads to the rate law given in eq 20 (see Appendix).

$$-\frac{d[Ru(sar)^{2+}]}{dt} = [k_0 + (k_0k_2k_3/k_5)^{1/2}][Ru(sar)^{2+}][O_2] \qquad (20)$$

The larger, pH-independent rate constant observed at high pH is thus ascribable to the additional reaction pathway presented by reactions 17 and 18, in which O_2^- cycles as a catalyst for the reduction of O_2 by $Ru(sar)^{2+}$ in a kind of chain reaction. Reactions 17 and 19 are written as hydrogen atom transfers because O_2^{2-} is too energetic a species to be accessible from an outer-sphere electron-transfer reaction between $Ru(sar)^{2+}$ and O_2^-, and protonation of O_2^- prior to its reaction with $Ru(sar)^{2+}$ is inconsistent with the observed pH independence of the rate constant k_{tot} at pH >10.

The observed increase in k_{tot} near pH 4.8 (Figure 3) is therefore attributable to the second term in the brackets in eq 20. That this term should be significantly larger than k_0 (note that $k_0 = k_{tot}$ at low pH) is reasonable if it is assumed that k_2 and k_5 are not very different because of the smaller dependence on driving force of hydrogen atom transfer than of outer-sphere electron-transfer reactions and that k_3 is larger than k_0 because $E^f_{IV/III}$ for half-reaction 10 is known[13c] to be less positive than $E^f_{3/2}$ for half-reaction 8.

The rationalization proposed above requires that reaction 17 (and 19), in which O_2^- acts as an oxidant, proceed rapidly despite the general tendency of O_2^- to behave as a reductant instead of an oxidant.[9,11] To provide supporting evidence for this assertion, the reaction between $Ru(sar)^{2+}$ and O_2^- at pH 12 was monitored spectrophotometrically at 430 nm. Addition of finely powdered aliquots of KO_2 to a solution containing an excess of $Ru(sar)^{2+}$ produced instantaneous increases in the absorption to new steady values. The spectrum of the resulting solutions corresponded to that for $Ru^{IV}(sar(-2H^+))^{2+}$, and the lack of further changes after the addition of each portion of KO_2 demonstrated the absence of significant quantities of O_2 from disproportionation of O_2^- because the excess $Ru(sar)^{2+}$ present would have reacted with O_2 at a known rate (Table I) to produce further increases in the absorption at 430 nm. Thus, the rapid oxidation of $Ru(sar)^{2+}$ by O_2^- seems unambiguously established.

Kinetics at 2.5 < pH < 10. At intermediate pH values it is necessary to consider simultaneously all of the reactions included in Schemes I and II. Applying the steady-state approximation to both $([O_2^-] + [HO_2])$ and $([Ru(sar)^{3+}] + [Ru^{III}(sar(-H^+))^{2+}])$ leads to the rate law (see supplementary material)

$$-\frac{d[Ru(sar)^{2+}]}{dt} = \left(k_0 + k_3\frac{K_{III}}{K_{III} + [H^+]}\frac{[Ru(III)]}{[Ru(sar)^{2+}]}\right)[Ru(sar)^{2+}][O_2] \qquad (21)$$

where $[Ru(III)] \equiv [Ru(sar)^{3+}] + [Ru^{III}(sar(-H^+))^{2+}]$.

It is clear from eq 21 that simple second-order kinetics are not to be expected in the general case. Instead, the observed rate constant, k_{tot} (eq 22), will depend on the pH and the reactant

$$k_{tot} = k_0 + k_3\frac{K_{III}}{K_{III} + [H^+]}\frac{[Ru(III)]}{[Ru(sar)^{2+}]} \qquad (22)$$

concentrations. To estimate the magnitude of the expected variations in k_{tot}, it is necessary to evaluate [Ru(III)]. Doing so (see supplementary material for the derivation) leads to the cubic equation

$$[Ru(III)]^2\left[[Ru(III)] + \alpha\gamma + \frac{k_3}{k_d}\beta\right] = \frac{k_0}{k_d}\alpha^2\beta\gamma \qquad (23)$$

where

$$\alpha = \frac{K_{III} + [H^+]}{K_{III}}[Ru(sar)^{2+}]$$

$$\beta = \frac{K_{III} + [H^+]}{[H^+]}[O_2]$$

$$\gamma = \frac{k_1[H^+] + k_2K_{HO_2}}{k_4[H^+] + k_5K_{HO_2}} = \frac{\frac{k_1}{k_2}[H^+] + K_{HO_2}}{\frac{k_4}{k_2}[H^+] + \frac{k_5}{k_2}K_{HO_2}}$$

Instead of dealing with the complex expressions resulting from the general solution of eq 23, it is illustrative to consider the limiting cases corresponding to the successive dominance of the three terms inside the brackets on the left-hand side of eq 23. At sufficiently high pH $k_3\beta/k_d$ will be orders of magnitude larger than both [Ru(III)] and $\alpha\gamma$ and the combination of eq 22 and 23 reduces to eq 24. This corresponds to the limiting behavior

$$k_{tot} = k_0 + \left(\frac{k_0k_2k_3}{k_5}\right)^{1/2} \quad (24)$$

at high pH as described above (cf. eq 20).

When [Ru(III)] is much larger than $\alpha\gamma$ and $k_3\beta/k_d$, it follows that

$$k_{tot} = k_0 + k_3\left(\frac{k_0K_{III}\gamma[O_2]}{k_d[H^+][Ru(sar)^{2+}]}\right)^{1/3} \quad (25)$$

and when $\alpha\gamma$ is much larger than [Ru(III)] and $k_3\beta/k_d$

$$k_{tot} = k_0 + k_3\left(\frac{k_0K_{III}[O_2]}{k_d[H^+][Ru(sar)^{2+}]}\right)^{1/2} \quad (26)$$

For both the second and the third case k_{tot} is predicted to exhibit a weak direct and inverse dependence on $[O_2]$ and $[Ru(sar)^{2+}]$, respectively, and in the most general case, with all terms in eq 23 contributing, the same qualitative behavior is expected. This is in good accord with the observed behavior. For example, note the trends in k_{tot} shown by the data in Table I at pH 6.2. This agreement helps to foster our confidence in the proposed mechanism.

To provide a more quantitative analysis of the kinetic data, the apparent second-order rate constants, k_{tot}, evaluated from eq 4–6 were fitted to eq 22 by using $K_{III}k_d = 37\ s^{-1}$ (eq 2) and the value of k_3 calculated from eq 27, where k_b is the limiting value of k_{tot}

$$k_3 = \frac{k_5}{k_0k_2}(k_b - k_0)^2 \quad (27)$$

obtained at high pH (eq 24). $[Ru(sar)^{2+}]$ was taken as half the initial concentration, and [Ru(III)] in eq 23 was evaluated by an iterative procedure based on eq 28. The remaining unknown

$$[Ru(III)]_0 = \left(\frac{\frac{k_0}{k_d}\alpha^2\beta\gamma}{\alpha\gamma + \frac{k_3}{k_d}\beta}\right)^{1/2}$$

$$[Ru(III)]_{n+1} = \left(\frac{\frac{k_0}{k_d}\alpha^2\beta\gamma}{[Ru(III)]_n + \alpha\gamma + \frac{k_3}{k_d}\beta}\right)^{1/2} \quad (28)$$

parameters, K_{III}, k_5/k_2, k_4/k_2, and k_1/k_2, were adjusted by a least-squares refinement to obtain the best agreement between the observed and calculated pH dependence of k_{tot}. Attempts to float all four parameters simultaneously suffered from high correlation between k_4/k_2 and k_1/k_2. To circumvent this problem, k_1/k_2 was kept constant and the fitting procedure was used to evaluate the other three parameters. The calculation was then repeated with a new value of k_1/k_2, and after each cycle the calculated dependences of k_{tot} on pH were compared with the experimental data. Reasonably satisfying agreement was obtained for the following range of the adjusted parameters: pK_{III} = 6.2–6.4; k_5/k_2 = 40–80; $k_4/k_2 = 5 \times 10^3$–5×10^4; k_1/k_2 = 10–10^2. Examples of calculated and observed values of k_{tot} with use of parameters from this range are listed in the supplementary material. The values of k_{calcd} listed in Table I were obtained by employing a specific set of parametric values; pK_{III} = 6.3; k_5/k_2 = 66; $k_4/k_2 = 1.9 \times 10^4$, k_1/k_2 = 60. The largest difference between the values of k_{tot} and k_{calcd} in Table I appears between pH 7 and 10, where the calculation predicts that k_{tot} should approach the limiting, high-pH value, k_b, more rapidly than is observed. However, the maximum difference is only ca. 30%. By combination of the estimates of the parameters given above with eq 27 and the previously measured parameters (eq 8, 9, 10, and 2) the following additional kinetic and equilibrium parameters were evaluated: $k_4/k_1 \approx 4 \times 10^2$; $k_4/k_5 \approx 2 \times 10^2$; k_3 = (3–6) $\times 10^4\ M^{-1}\ s^{-1}$; k_d = (6–9) $\times 10^7\ M^{-1}\ s^{-1}$; K_d = (1–1.5) $\times 10^4$. The formal potential for half-reaction 10 can then be calculated to be 0.04–0.06 V vs NHE.

It should be noted that the calculated pH dependence of k_{tot} did not match the observed dependence under the assumption that the dependence of the rate of the H atom transfer reaction was little influenced by driving force; i.e., $k_2 \approx k_5$. The larger value of k_5/k_2 needed to obtain the best fit ($k_5/k_2 \approx 66$) indicated a significant dependence of the rates of reactions 17 and 19 on the driving force. The net effect is that the observed increase in k_{tot} as the pH increases must be attributed to the more rapid regeneration of the catalyst, O_2^-, by reaction 18 than its removal by reaction 19.

Discussion

The estimate of the acid dissociation constant for the $Ru(sar)^{3+}$ complex, pK_{III} = 6.2–6.4, is one important result of this study. It represents an enormous enhancement in the acidity of a proton on a secondary amine nitrogen atom upon the coordination of that N atom to a Ru(III) center. For example, the corresponding pK for $Ru(NH_3)_6^{3+}$ is 12.4.[16]

A second noteworthy result is the demonstration of the catalysis of the autoxidation of $Ru(sar)^{2+}$ by the O_2^- generated in the first step of the proposed reaction mechanism. Although indirect, the evidence for the important intermediacy of O_2^- was compelling. No other mechanistic scheme we could conceive was as satisfactory in accounting for the observed pH dependence of the rate of the autoxidation while accommodating simple second-order behavior under limiting acidic or alkaline conditions and the relatively weak deviations from second-order kinetics observed at intermediate pH values. Additional evidence of the important catalytic role played by O_2^- in the proposed mechanism was the sharp decrease in rate that resulted when small amounts of the enzyme superoxide dismutase (SOD)[23] were added to the reaction solution. SOD catalyzes the dismutation of superoxide at close to the diffusion-controlled rate.[24] At pH 10.1 the rate of the autoxidation of 4×10^{-5} M $Ru(sar)^{2+}$ by 1.1×10^{-3} M O_2 decreased by 50% upon the addition of ca. 1.3×10^{-8} M SOD.

The proposal that O_2^- acts as an effective oxidant toward both $Ru(sar)^{2+}$ and $Ru^{III}(sar(-H^+))^{2+}$ by abstracting a hydrogen atom is somewhat surprising in view of the stability of O_2^- toward reasonably efficient hydrogen atom donors such as dimethyl sulfoxide. The implication is that the metal center that is coordinated to the nitrogen atom from which the hydrogen comes is quite effective in enhancing the hydrogen atom transfer process. A similar interpretation was offered recently by Bakac et al.[2a] in a study of the oxidation of $Co(sep)^{2+}$ by O_2^-. That we encountered analogous chemistry with the $Ru(sar)^{2+}$ complex suggests that hydrogen atom transfer may be a general reaction pathway accessible to O_2^- with suitable metal-activated ammine complexes as coreactants.

HO_2 and O_2^- both react more rapidly with the more strongly reducing $Ru^{III}(sar(-H^+))^{2+}$ than with $Ru^{II}(sar)^{2+}$. The difference

(16) Navon, G.; Waysbort, D. *J. Chem. Soc., Chem. Commun.* **1971**, 1410.

Scheme III

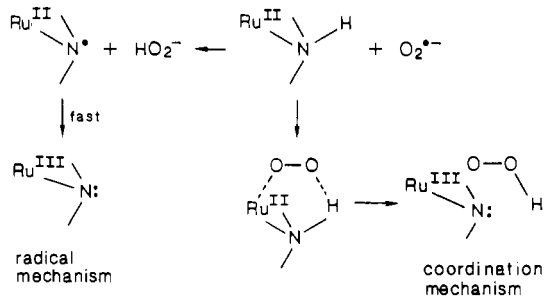

in reactivity is greater for HO_2 than for O_2^-, which is in qualitative agreement with our assignment of the former reaction as an outer-sphere electron transfer and the latter as a hydrogen atom transfer that is less responsive to (though not unaffected by) changes in driving force. We examined the reaction between $Ru(sar)^{2+}$ and O_2^- at pH 11.7 in stopped flow experiments similar to those described by Bradic and Wilkins.[3] The resulting value of k_2 was $(1.2 \pm 0.6) \times 10^6$ M^{-1} s^{-1}.[17]

Mechanism of H Atom Transfer. The transfer of a hydrogen atom from $Ru(sar)^{2+}$ to O_2^- might proceed by a pathway in which a complex containing Ru(II) and a nitrogen-based radical would be an intermediate that turned into $Ru^{III}(sar(-H^+))^{2+}$. Alternatively, an inner-sphere mechanism can be imagined in which coordination of O_2^- to the ruthenium center generates a seven-coordinate intermediate that decomposes to HO_2^- and $Ru^{III}(sar(-H^+))^{2+}$ in a concerted electron–proton transfer step. The essential difference between the two mechanisms lies in the configuration of the reactants during the electron-transfer step (Scheme III). In the first (radical) mechanism electron transfer occurs within a N–H–O fragment while in the second (coordination) mechanism it occurs between O_2^- and the Ru(II) center to which it is coordinated. The accompanying proton transfer, which leads to the net transfer of a hydrogen atom, occurs to the electron-accepting oxygen atom of O_2^- in the first mechanism but to the uncoordinated oxygen atom in the second mechanism.

The available data do not allow a choice to be made between these two mechanisms. The mechanism involving a nitrogen-based radical has the advantage that no expansion of the coordination sphere of Ru(II) is required. However, the radical intermediate, which resembles an electronically excited state resulting from the LMCT band for $Ru^{III}(sar(-H^+))^{2+}$ that appears at ~450 nm,[13c] would be highly reactive. One might expect the rate of reactions that follow this mechanism to be less sensitive to changes in the driving force than the alternative mechanism given in Scheme III.

The expanded coordination about Ru(II) required by the second mechanism in Scheme III is sterically unfavorable because the encapsulating ligand is packed very tightly about the metal center. However, factors that would favor such a mechanism are the general high affinity of O_2^- for metal ions[7] and the unusual chemistry previously observed for coordinatively saturated Ru(II) amine complexes, including protonation of the metal[13c,18] and electrophilic attack by NO^+.[19] The reaction with O_2^- could be regarded as a concerted electron–proton transfer in which transfer of the electron "leads" the reaction: As the positive charge on the metal increases, the N–H proton becomes more labile and is ultimately transferred to the increasingly basic uncoordinated oxygen atom. The electronic energies involved are expected to be lower than for the radical mechanism because the reaction does not proceed through an "excited state" structure. The significantly larger rate constant for the reaction of O_2^- with the more strongly reducing $Ru^{III}(sar(-H^+))^{2+}$ compared with that for the reaction with $Ru^{II}(sar)^{2+}$ is more readily accommodated by the driving-force-sensitive coordination mechanism than the less sensitive radical mechanism. Additional supporting factors include the general tendency of Ru(III) to react via associative pathways[20] and the likely greater lability of $Ru^{III}(sar(-H^+))^{2+}$ with respect to N–H exchange than of $Ru^{II}(sar)^{2+}$.[13c]

Kinetic Isotope Effect. The pH-independent rate constant measured at high pH depends upon the ratio of rate constants for two H atom transfer reactions (eq 20) so that the small measured ratio of $k_{tot}(H_2O)/k_{tot}(D_2O)$ at pH 12 (Table I) was not unexpected. It is difficult to distinguish between the contributions to this ratio arising from primary isotope effects on k_2 and k_5 and those arising from changes in the solvent[21] to which the strongly hydrogen-bonding[9] O_2^- is exposed. A similarly small isotope effect (2.1) was measured[2a] in the oxidation of $Co^{II}(sep)^{2+}$ by O_2^-, which implies that proton transfer to the relatively weak base, O_2^-, lags somewhat behind the electron transfer that converts it into the much more basic O_2^{2-} anion.

Self-Exchange Rates. An estimate of the self-exchange rate constant for the $Ru^{IV/III}(sar(-H^+))^{3+/2+}$ couple can be obtained by using the values of k_{-d} (6.2×10^3 M^{-1} s^{-1}, eq 2), k_d ($(6–9) \times 10^7$ M^{-1} s^{-1}), and the self-exchange rate constant for the $Ru(sar)^{3+/2+}$ couple (1.2×10^5 M^{-1} s^{-1}).[13b] Application of the Marcus cross relationship to the disproportionation reaction leads to a value of $(7–14) \times 10^6$ M^{-1} s^{-1} for the self-exchange of the deprotonated Ru(IV/III) couple. This is significantly larger than the corresponding constants for ruthenium complexes with saturated ligands and suggests that the pair of electrons resident on the nitrogen atom of a deprotonated, coordinated amine group can provide a very efficient pathway for electron transfer.

The value of k_0, 1.4 M^{-1} s^{-1}, obtained at low pH for the autoxidation of $Ru(sar)^{2+}$ can be employed in the Marcus cross relationship to calculate the self-exchange rate constant for the O_2/O_2^- couple by using the formal potential and self-exchange rate constant for the $Ru(sar)^{3+/2+}$ couple (0.29 V and 1.2×10^5 M^{-1} s^{-1},[13b] respectively) and the formal potential for the O_2/O_2^- couple (–0.15 V; standard state of 1 M O_2[22]). The value obtained is 4×10^3 M^{-1} s^{-1}. A similar calculation based on the rate constant for the autoxidation of the $Ru^{III}(sar(-H^+))^{2+}$ complex ($k_3 = (3–6) \times 10^4$ M^{-1} s^{-1}), the formal potential of the $Ru^{III}(sar(-H^+))^{3+/2+}$ couple (0.04–0.06 V), and the values of k_d and k_{-d} for reaction 2 ($(6–9) \times 10^7$ and 6×10^3 M^{-1} s^{-1}, respectively) leads to a value of 4×10^5–4×10^6 M^{-1} s^{-1} for the O_2/O_2^- self-exchange constant. This sort of discrepancy among calculated self-exchange constants is well-known in the cross reactions of O_2 and O_2^- with a variety of different reaction partners[4] and emphasizes the caution that must be used in attempting to apply the Marcus cross relationship to reactant couples as structurally different as O_2/O_2^- and transition-metal complexes.

The value of k_0 for the autoxidation of $Ru(sar)^{2+}$ falls on, while k_3 for the autoxidation of $Ru(sar(-H^+))^{2+}$ falls well off, the linear free energy relationship established by Stanbury et al.[1a] in a study of the autoxidations of a series of ruthenium(II) amine complexes. However, such linear relationships are neither necessary nor sufficient to demonstrate adherence to the Marcus cross relationship by the couples involved so that the nonconforming behavior of the $Ru(sar(-H^+))^{3+/2+}$ couple is not necessarily anomalous.

Conclusions

The reactivity pattern encountered in this study of the autoxidation of $Ru(sar)^{2+}$ (and its oxidation products) differs from

(17) Bernhard, P.; Anson, F. C., submitted for publication in *Inorg. Chem.*
(18) (a) Ford, P. C.; Kuempel, J. R.; Taube, H. *Inorg. Chem.* **1968**, *7*, 1976. (b) Shepherd, R. E.; Taube, H. *Inorg. Chem.* **1973**, *12*, 1392.
(19) Armor, J. N.; Scheidegger, H. A.; Taube, H. *J. Am. Chem. Soc.* **1968**, *90*, 5928.
(20) (a) Matsubara, T.; Creutz, C. *J. Am. Chem. Soc.* **1978**, *100*, 6255; *Inorg. Chem.* **1979**, *18*, 1956. (b) Fairhurst, M. T.; Swaddle, T. W. *Inorg. Chem.* **1979**, *18*, 3241. (c) Rapaport, I.; Helm, L.; Merbach, A. E.; Bernhard, P.; Ludi, A. *Inorg. Chem.* **1988**, *27*, 873.
(21) Unfortunately, the H/D exchange in $Ru(sar)^{2+}$ is quite rapid ($t_{1/2} \approx$ 100 s) and is increased greatly by traces of $Ru(sar)^{3+}$ so that measurements in H_2O with the N-deuteriated complex are not feasible.
(22) (a) Ylan, Y. A.; Czapski, G.; Meisel, D. *Biochim. Biophys. Acta* **1976**, *430*, 209. (b) Sawada, Y.; Iyanugi, T.; Yamazaki, I. *Biochemistry* **1975**, *14*, 3761.
(23) McCord, J. M.; Fridovich, I. *J. Biol. Chem.* **1969**, *244*, 6049.
(24) Rotilio, G.; Bray, R. C.; Fielden, E. M. *Biochem. Biophys. Acta* **1972**, *268*, 605.

that described in most previous studies on autoxidations of transition-metal complexes. The extraordinarily high Brønsted acidity of $Ru^{III}(sar)^{3+}$ and the facile disproportionation of the deprotonated complex were two novel features in the reaction chemistry that contributed to the unusual pH dependence of the autoxidation rate. Similar behavior might also be encountered with other ruthenium complexes that are sufficiently stable at high pH. The unusual ability of O_2^- to act as an oxidant by accepting a hydrogen atom is likely a reflection of a great enhancement in the hydrogen-donating ability of the sar ligand induced by its coordination to ruthenium because O_2^- is not a particularly effective hydrogen atom acceptor. Our results and those of Bakac et al.[2a] suggest that oxidations of transition-metal complexes by O_2^- via H atom transfer may be more common than previously thought. This is a speculation that seems worthy of further tests.

Acknowledgment. The work was supported by the National Science Foundation. Helpful discussions with Prof. J.-M. Savéant are a pleasure to acknowledge.

Appendix

The rate laws at the limits of high and low acidity can be derived as follows.

Acidic Limit (See Scheme I). When $[H^+] \gg K_{III}$ and K_{HO_2}, all of the Ru(III) will be present as $Ru(sar)^{3+}$ and all of the superoxide will be present as HO_2. Then

$$\frac{d[Ru(sar)^{2+}]}{dt} = -k_0[Ru(sar)^{2+}][O_2] - k_1[Ru(sar)^{2+}][HO_2] + \frac{k_d K_{III}}{[H^+]}[Ru(sar)^{3+}]^2 \quad (A1)$$

$$\frac{d[Ru(sar)^{3+}]}{dt} = k_0[Ru(sar)^{2+}][O_2] + k_1[Ru(sar)^{2+}][HO_2] - 2\frac{k_d K_{III}}{[H^+]}[Ru(sar)^{3+}]^2 - \frac{k_4 K_{III}}{[H^+]}[Ru(sar)^{3+}][HO_2] \quad (A2)$$

$$\frac{d[HO_2]}{dt} = k_0[Ru(sar)^{2+}][O_2] - k_1[Ru(sar)^{2+}][HO_2] - \frac{k_4 K_{III}}{[H^+]}[Ru(sar)^{3+}][HO_2] \quad (A3)$$

The steady-state approximation for both $[Ru(sar)^{3+}]$ and $[HO_2]$ leads to eq A4. Introduction of eq A4 into eq A1 leads to eq

$$\frac{k_d K_{III}}{[H^+]}[Ru(sar)^{3+}]^2 - k_1[Ru(sar)^{2+}][HO_2] = 0 \quad (A4)$$

16 in the text.

Basic Limit (See Scheme II). When $[H^+] \ll K_{III}$ and K_{HO_2}, essentially all of the Ru(III) will be present as $Ru^{III}(sar(-H^+))^{2+}$ and the superoxide will be present as O_2^-. Then

$$\frac{d[Ru(sar)^{2+}]}{dt} = -k_0[Ru(sar)^{2+}][O_2] - k_2[Ru(sar)^{2+}][O_2^-] \quad (A5)$$

$$\frac{d[Ru^{III}(sar(-H^+))^{2+}]}{dt} = k_0[Ru(sar)^{2+}][O_2] + k_2[Ru(sar)^{2+}][O_2^-] - k_3[Ru^{III}(sar(-H^+))^{2+}][O_2] - k_5[Ru^{III}(sar(-H^+))^{2+}][O_2^-] \quad (A6)$$

$$\frac{d[O_2^-]}{dt} = k_0[Ru(sar)^{2+}][O_2] - k_2[Ru(sar)^{2+}][O_2^-] + k_3[Ru^{III}(sar(-H^+))^{2+}][O_2] - k_5[Ru^{III}(sar(-H^+))^{2+}][O_2^-] \quad (A7)$$

The steady-state approximation for both $[Ru^{III}(sar(-H^+))^{2+}]$ and $[O_2^-]$ and the sum and difference of eq A6 and A7 leads to eq A8 and A9, respectively. Simultaneous solution of eq A8 and

$$k_3[Ru^{III}(sar(-H^+))^{2+}][O_2] - k_2[Ru(sar)^{2+}][O_2^-] = 0 \quad (A8)$$

$$k_0[Ru(sar)^{2+}][O_2] - k_5[Ru^{III}(sar(-H^+))^{2+}][O_2^-] = 0 \quad (A9)$$

A9 yields eq A10 and A11. Substitution of eq A11 into eq A5

$$[Ru^{III}(sar(-H^+))^{2+}] = \frac{k_2[Ru(sar)^{2+}][O_2^-]}{k_3[O_2]} \quad (A10)$$

$$[O_2^-] = \left(\frac{k_0 k_3}{k_2 k_5}\right)^{1/2}[O_2] \quad (A11)$$

leads to eq 20 in the text.

Supplementary Material Available: Derivation of the general mechanism for the autoxidation of $Ru(sar)^{2+}$ and a table of the observed and calculated rate constants k_{tot} for various parameter sets (8 pages). Ordering information is given on any current masthead page.